THE HUNT FOR LEAKY ELEVATED INFRASONIC WAVEGUIDES

Milton A. Garcés, Mark Willis, Claus Hetzer, and S. Businger

University of Hawaii, Manoa

Sponsored by Army Space and Missile Defense Command

Contract No. DTRA01-01-C-0077

ABSTRACT

The ability to locate explosive events with infrasound pivots on our understanding of the temporal and spatial scales of atmospheric variability that define the propagation paths that sound waves may take from the source to the receiver. Source location analyses of bolide events suggest that high-altitude sources may efficiently ensonify elevated waveguides in the stratosphere, and that this acoustic energy may leak to the ground by diffraction and scattering. There is also a precedent for ground-based explosive sources that may yield stratospheric returns even when sound is propagating against the prevailing winds. Microbaroms are infrasonic waves generated by nonlinear interactions of ocean surface waves traveling in nearly opposite directions with similar frequencies. Such interactions commonly occur between ocean waves with approximately 10-second periods, which are abundant in the open oceans and correspond to the observed 0.2 Hz infrasonic spectral peak. Although microseisms and microbaroms share a common source, microseisms in the ground and oceans are generated by the vertical component and microbaroms are generated by the near horizontal component of the source radiation pattern. In contrast to microseisms, microbarom signals are also strongly influenced by the atmospheric winds. We compared microbarom signals observed at Hawaii in 2003 with the Wavewatch 3 ocean wave model and the Naval Research Laboratory (NRL) Ground-to-Space (G2S) atmospheric specification. The arrival azimuths of coherent microbarom signals observed in Hawaii are associated with high ocean wave activity in the Pacific Basin, the dominant wind directions in the troposphere, stratosphere, and mesosphere, and the thermal structure of the atmosphere. Some of the seasonal trends in the microbarom observations can be explained by the winds in the stratosphere and lower mesosphere, while some of the daily variability can be explained by the winds in the troposphere and lower stratosphere. However, coherent energy from powerful swells may overcome the wind-carried microbarom signals and arrive to the station through thermospheric ducting. Our observations suggest that either (1) the wind speeds in the troposphere, stratosphere and lower mesosphere may be underestimated in atmospheric models or (2) leaky elevated infrasonic waveguides are persistent propagation paths that should be investigated in more detail. Although ocean swells have been previously used as a natural source for continuous measurements of atmospheric winds over long horizontal ranges, recent advances in measurement and modeling techniques can provide new insight on this complex but tractable method for continuous, passive acoustic tomography of the atmosphere.

OBJECTIVE

The aim of this work is to characterize microbarom signals observed in the Pacific and model the source processes that generate these signals, with the aim of determining infrasonic detection thresholds in the microbarom frequency range. In the process of differentiating the effects of swells and winds on infrasonic wave generation and propagation, we also found that microbarom signals may be readily used to test and validate atmospheric winds and temperature specifications in the lower, middle and upper atmosphere. Such accurate atmospheric specifications are essential for the development of accurate infrasonic location algorithms.

RESEARCH ACCOMPLISHED

Introduction

A large fraction of the ambient infrasonic field observed at I59US, Hawaii, is related to pervasive signals known as microbaroms. Microbaroms are observed as a continuous atmospheric pressure oscillation with most of its energy between 0.1 and 0.5 Hz (Figure 1). Microbaroms are detected at the I59US arrays as coherent bursts with durations of minutes and have a root mean square (RMS) amplitude varying between approximately 10 mPa and 100 mPa. For infrasonic stations near the ocean, microbaroms comprise the low-wind noise floor. The microbarom peak is in the midst of the detection region for 1-kt nuclear explosion tests, and thus microbaroms can obscure an important signal of interest.

Microbaroms were first observed by Benioff and Gutenberg (1939) on an electromagnetic microbarograph at the Seismological Laboratory of the California Institute of Technology. At the time of their studies, there was no accepted hypothesis for microbaroms or their better-known seismic counterparts, microseisms. Longuet-Higgins (1950) was the first to recognize and develop a theory for the excitation of microseisms by ocean waves. Studies by Saxer (1945, 1954), Daniels (1952, 1962), Donn and Posmentier (1967), Donn and Naini (1973) and Rind (1980) confirmed that microbarom and microseism sources are related to strong storms over the ocean and the resulting high seas. The accepted physical mechanism for microbarom and microseism generation is the nonlinear interactions of ocean surface waves traveling in nearly opposite directions with similar frequencies (e.g. Arendt and Fritts, 2000). Microbaroms exhibit frequencies twice that of the individual ocean waves and amplitudes proportional to the product of the energy of the opposing wave trains. However, while microseisms propagate through the ground as a result of vertical excitation through the ocean, microbaroms propagate to infrasonic stations after horizontal propagation through the atmosphere (Tabulevich, 1995). Thus seismic and infrasonic measurements sample complementary portions of the total radiated source field. Yet microbaroms will be primarily affected by the dynamic temperature and wind structure of the atmosphere, whereas microseisms will be propagated through the relatively static geologic structure of the Earth. This paper seeks to explain in more detail the effects of atmospheric temperature and winds on the spatial, temporal, and spectral distribution of coherent and incoherent microbarom energy.

A typical power spectral density plot for I59US is shown in Figure 1. During the winter season, when surf is highest, the frequency band above 2 Hz is dominated by sound from breaking ocean waves (Garcés *et al.*, 2003). The large, broad peak between 0.1 and 1 Hz corresponds to coherent and incoherent microbarom energy arriving from all possible source regions in the Pacific. The microbarom peak usually has a maximum at 0.2 Hz, corresponding to the 10s periods common to open-ocean swells, but may have a secondary peak between approximately 0.12 and 0.15 Hz or the peak may appear to broaden to include this frequency band. As discussed in Willis (2004), the lower frequency component corresponds to large, long-period swells that can be sufficiently energetic to dominate the coherent infrasound field in the microbarom band. Previous work (Daniels, 1952; Donn and Rind, 1971; Rind, 1978) related microbarom amplitude variability to solar tide fluctuations in the thermosphere during winter and stratospheric wind strength during summer. Their studies concentrated on the results from an infrasound station in the eastern U.S. that was primarily exposed to microbaroms arriving from the North Atlantic. Le Pichon *et al.* (2003) showed a correlation between the prevailing direction of the stratospheric winds and microbarom arrival azimuths observed by southern hemisphere stations. These austral stations would primarily observe the ocean swells driven by southern hemisphere typhoons and the continuous circumpolar winds. In this study we investigate microbaroms arriving at Hawaii from anywhere in the Pacific Ocean, and we present a relationship between the arrival direction of coherent microbarom energy and the dominant wind direction in regions of the troposphere,

stratosphere, and lower mesosphere. In addition, we postulate that microbaroms generated by energetic swells may refract in the thermosphere to arrive at a station from any direction.

Microbarom observations at I59US during 2002–2003

The Progressive Multi-Channel Correlation (PMCC) algorithm of Cansi *et al.* (1995) is the primary detection system used at I59US. PMCC uses the cross-correlation between various groupings of three sensors to estimate the consistency of the lag-closure (Cansi and Klinger, 1997). A microbarom detection is only registered if the consistency is below 0.5s within the 0.1–0.5 Hz passband. The microbarom event processing scheme utilizes an analysis of overlapping windows of data (length–90s, overlap–70s). PMCC is used to detect coherent infrasonic energy across the array, which allows the apparent horizontal phase speed, arrival azimuth, and amplitude of the detected arrivals to be extracted. Infrasonic power spectral densities (Figure 1) are used to study the spectral structure in the microbarom frequency range. The power spectral densities were computed using the modified periodogram method (Madisetti and Williams, 1998) with a 102.4s Hanning window (2^{11} samples) and a 50% overlap. Power spectra include the combination of both coherent and incoherent microbarom contributions. Infrasonic power spectral densities at I59US exhibit a quasi-permanent peak around 0.2 Hz (Figure 1). This corresponds to the abundance of microbarom energy produced by opposing ocean waves containing periods of approximately 10s. Occasionally, the peak will broaden or split at slightly lower frequencies (approximately 0.12 to 0.15 Hz) when the conditions are just right to where strong storm systems are producing an abundance of interacting long period swell energy.

Strong microbarom signals tend to arrive from regions of marine storminess because they can produce high amplitude ocean waves converging from opposite directions. By using wave spectra output by the Wavewatch (WW3) model (Tolman et al., 2002) in conjunction with the infrasonic source formulation of Garcés et al. (2003), Willis (2004) confirmed that strong microbarom source regions in the Pacific often occur in the wake regions of both mid-latitude and tropical cyclones, where swell spectra are confused with multidirectional components created ahead of and behind the surface low center (Figure 2). This research also showed that strong signals can originate outside of storm wake regions (occasionally 1,000–3,000 km away from the wave producing winds), especially when multiple storms are present. The wake region microbarom generation theory is discussed in Ponomaryov et al. (1998) and converging wave trains of opposite directions were also observed in the wake of Hurricane Bonnie (Wright et al, 1998).

Coherent microbarom arrival azimuths and amplitudes at the I59US site during 2002–2003 show an annual cycle (Figure 3). During the months from June through September microbarom arrivals generally come from east (55°–130°) or south (160°–220°) directions. The concentration of east arrivals is much stronger than the south arrivals during this time. Months October through March show an abundance of arrivals from 230°–360° with a peak from northwesterly directions. Arrivals during April, May, late September and early October appear to arrive from a variety of different azimuths with no distinct peak noted. Annual arrivals correspond to dominant storm activity in the Pacific Basin but are also affected by topographic shadowing and zonal and meridional winds throughout the atmosphere.

A total of 21,459 coherent microbarom arrivals reached I59US in 2003. Of these arrivals 9,334 (43%), came from 270°–315°. The second highest 45 degree directional bin, 225°–270°, contained 4,211 (19.6%) microbarom arrivals during 2003. 2606 arrivals (12%) came from 45°–90°, 1605 (7.5%) from 315°–360°, 1599 (7.5%) from 180°–225°, 1,168 (5.4%) from 0°–45°, 549 from 90°–135°, while only 377 arrivals came from azimuths 135°–180°.

During the first quarter of 2003 (containing months December 2002, January and February 2003), 98% of the microbarom arrivals came from azimuths 225°–360°. The second quarter of 2003 (March, April, May) shows a similar directional dependence with 81% of the arrivals coming from 225°–360°. However, stronger signatures from 0°–90° (13%) and 180°–225° (4%) were evident in the second quarter, than in first quarter.

A very different pattern of microbarom arrival azimuths was observed during the boreal summer months. 70% of the arrivals during June, July, and August came from 0°–135° while 26% came from 135°–225°. Arrivals at I59US during the fall months of fourth quarter (September, October, November) show a very similar pattern to the springtime (second quarter) arrivals–with 72% coming from 225°–360°, 13% from 0°–90°, and 10% from 180°–225°.

The effect of temperature and wind on the reception of microbarom signals

The temperature and winds in the atmosphere determine where sound waves travel (e.g. Cox et al., 1954). Infrasound can propagate for long ranges in waveguides defined by the thermal and wind structure of the atmosphere. Along the downwind direction, infrasonic energy may be trapped between the ground and the troposphere and lower stratosphere (tropospheric ducting), and between the ground and the stratosphere and lower mesosphere (stratospheric ducting). However, if the winds are not sufficiently strong, these tropospheric and stratospheric waveguides do not reach the ground. From a ray theory perspective, such elevated waveguides would not be able to transfer energy to ground-based recording stations. But in practice, such waveguides may leak energy to the ground through diffraction and scattering (Garcés et al., 2002b). Due to the high temperatures at the thermosphere, infrasonic energy is always refracted back to the ground by the thermosphere (thermospheric ducting), although the attenuation is stronger for these paths.

In order to produce atmospheric specifications for infrasonic propagation studies, NRL G2S model (Drob et al, 2003) was run to produce a self-consistent dataset extending from January 1, 2003 to March 29, 2004. Global spectral coefficients of wind, temperature, and density were produced at 6-hour time intervals. These coefficients have a triangularly truncated spectral order of 72 (T–72) resulting in an effective output resolution of approximately 2.25 degrees.

From the Earth's surface to 10 mb (0 to 35 km), we use 1x1 degree operational global aviation weather forecasts from the National Oceanic and Atmospheric Administration (NOAA) National Centers for Environmental Predication (NCEP). From 1 to 0.4 mb (20 to 55 km), we use the 1.0 x 1.5 global assimilative analysis from the NASA Goddard Space Flight Center, Global Modeling and Assimilation Office (GSFC-GMAO). This data set is limited distribution but available for basic scientific research. The upper atmosphere conditions (50 to 170 km) are specified by the HWM/MSIS models, which use the 3-hour and daily geomagnetic activity (Ap) and solar EUV flux (F10.7) indices from the NOAA space environment center (SEC). The trade winds typical of the tropical regions are generally limited to the lower 4 km of the atmosphere, and may be excessively averaged by the 1 km grid of the G2S specifications.

In order to investigate the effect of atmospheric winds on microbarom propagation, the wind speed and wind arrival azimuth (Figure 4) were extracted from the G2S global grids at a vertical profile above the Hawaii infrasound station. We evaluated Figures 1 and 2 at a fixed time (18 h GMT) to eliminate the variability induced in the thermosphere by the solar tides (Garcés et al., 2000). Although most of the tropospheric variability appears to be governed by storms, it is possible to observe clear seasonal patterns above 15 km. As will be discussed in the next section, the detection of coherent microbarom energy appears to be primarily dictated by the proximity of the source, the swell extent and size, and the predominant wind direction in specific regions of the atmosphere.

Microbaroms determined by swell size, wind strength, and source proximity

Modeling the radiation of infrasonic waves from the nonlinear interaction of ocean waves is far from trivial. Willis (2004) used the output of the WW3 model to produce a frequency-dependent synoptic plot of the microbarom source regions in the Pacific. His results show that microbarom sources with a frequency of 0.2 Hz form predominantly between two storms or in the lee of a storm, and are abundant in the Pacific. Thus a listening post in the midst of the ocean will be continuously bombarded by microbarom signals originating from multiple azimuths and ranges. When these signals arrive at an infrasonic array and are processed to find the most coherent arrivals, a competition ensues. Figure 5 shows as black dots all the coherent arrivals observed in Hawaii for 2003. These arrivals have an apparent horizontal phase velocity that is close to that of the sound speed at the ground, suggesting that the source energy was radiated very close to the horizontal. There is an obvious seasonal trend, with microbaroms arriving predominantly from the northwest in winter and south and northeast in summer. The prevailing wind directions between 50–70 kms are shown as red dots, and the winds between 10–20 kms are shown as blue dots in Figure 5. We can see that the seasonal pattern roughly coincides not only with the most energetic swell source regions but also with the prevailing wind directions in the selected layers. Microbaroms arriving from the south during summer, which would reach at the Hawaii array through multiple bounces between the thermosphere and the ground, would be affected by the solar tides in the upper atmosphere. As shown in Willis (2004), the summer arrivals appear to have a lower amplitude. During the shoulder periods of spring and fall,

arrivals are more evenly distributed along the compass (Willis et al., 2004), corresponding to the change in the wind patterns and a more equitable partition of swell energy between the northern and southern hemispheres. By using the G2S models to compute the wind-corrected effective sound speeds over Hawaii, the upper boundaries of the stratospheric ducts are predicted to reach as high as 70 km during winter, and as low as 60 km during summer. However, from April to May and September to October, stratospheric winds are light. and stratospheric waveguides are predicted to be elevated above the ground. Likewise, tropospheric winds at approximately 10 km are only sufficiently strong in January and February to consistently maintain a ground-reaching tropospheric waveguides. The lower panel of Figure 5 shows a close up of the upper panel for the months of January and February of 2003. These are often the most active swell months for the Hawaiian Islands. Some of the microbarom arrival azimuths in January and February track the tropospheric winds very well, corresponding to energy that would be refracted back to the ground between the 10–20 km height in the atmosphere, where there is very little attenuation. Likewise, energy ducted between the lower mesosphere and the ground would suffer very little attenuation and thereby retain a relatively large amplitude. However, some microbarom azimuths do not match the prevailing winds, as in the case of January 4–to 7, 2003. This case study corresponds to the largest swell event of 2003 (Garcés et al. 2003), is considered in detail by Willis (2004), and will be the subject of a separate paper. The marine storm responsible for this event produced high open ocean wave heights over a wide spectrum of frequencies between 0.05 and 0.1 Hz, and thus produced high microbarom source amplitudes between 0.1 and 0.2 Hz. High source amplitudes, coupled with lower attenuation and a larger correlation length at lower frequencies, would permit long-range propagation of this energy over large distances and preferential detection by an array.

Thus it is possible to explain the structure of ocean-related infrasound spectra observed in Hawaii (Figure 1) by attributing (1) a broad 2–5 Hz energy peak to breaking ocean waves (surf) in the littoral zone, (2) 0.2 Hz energy to the predominant 10s swell energy and (3) 0.1–0.2 Hz energy to 12s–20s period swells associated with powerful storms. The surf peak depends on the swell energy arriving near the array site, and in Hawaii surf sound appears to be propagated in the boundary layer and the troposphere. The coherent component of the main microbarom peak at 0.2 Hz depends on the prevailing winds and the amount of swell energy in the ocean. However, the energy of the main microbarom peak is the sum of coherent and incoherent components, and the amplitude of this peak may be related to the diurnal tides in the upper atmosphere (Rind, 1978). Coherent microbaroms in the approximately 0.12 to 0.2 frequency range may arrive from any direction where energetic long-period swells are interacting, and under certain circumstances may also be used to study the mesosphere and lower thermosphere (Garcés *et al.*, 2002a). Such thermospheric returns would explain southerly arrivals associated with the powerful southern hemisphere swells during the boreal summer.

CONCLUSIONS AND RECOMMENDATIONS

Microbaroms are generated wherever ocean surface waves traveling in nearly opposite directions with similar frequencies meet. This situation commonly occurs with ocean waves of periods near 10s, in particularly in storm wake regions. Thus, a quasi-permanent infrasonic spectral peak of 0.2 Hz is observed at I59US, as well as most infrasound stations in the world. In the case of an eastward-moving middle latitude storm, the south side of the storm will contain the strongest fetch lengths, durations, and intensities and thus higher wave heights and periods can be expected on the south of the center. It is rare for an eastward moving storm to produce long wave periods of 13s or more on the north side of the center unless the storm is a slow mover, large in diameter, and quite strong. Furthermore, since long period swells exhibit higher group velocities than short period swells, unless a storm is very large, symmetrical, and fast moving, the long period energy created ahead of a low center will often be dispersed and not have time to interact with any longer period energy that may be created behind the low center. This is especially true when the storm is moving slower than the group velocities of the long period ocean waves it produces. Steep, short period swells (< 8s) often dissipate within a few wavelengths due to whitecapping and angular spreading effects. This can prevent opposing wave trains of short periods from interacting. On the other hand, opposing wave trains of medium periods (8s–12s) are very likely in wake of both middle latitude and tropical cyclones, giving credence to the commonly observed infrasonic peak at 0.2 Hz. If there are long period swells created on the north side of the center, the amplitudes are normally small and thus the resulting infrasonic wave will also have small amplitude. Similarly, dissipating shorter period swells that may interact will also produce smaller amplitude infrasonic waves. This also helps explain the persistent infrasonic spectral peak at 0.2 Hz.

Coherent microbarom arrivals at I59US during 2003 suggest a relationship between microbarom arrival azimuth and dominant storm activity in the Pacific Basin (Figure 2). Boreal winter-time arrivals at I59US come from west and

northwest directions, while summer arrivals come primarily from east and south azimuths. Arrivals during the shoulder seasons are more evenly distributed around the compass. Microbaroms observed at I59US come primarily from regions where storm and wave activity are the strongest throughout the year, and the seasonal trend roughly coincides with the stratospheric wind patterns. The seasonal pattern of coherent microbarom amplitudes may be due to the closer distance of the source to the receiver during winter. Propagation path effects may also play a role, and will be addressed in a separate study. Figure 4 also shows evidence for acoustic shadowing by adjacent Mauna Loa and Hualalai volcanoes, which shelter the array from the trade winds. Reflections from the coastline may also contribute to a portion of the arrivals from 45° to 95° at I59US, especially during summer months when trade winds are present 80–90% of the time near the Hawaiian Islands (Sanderson, 1993).

Infrasound generated by the ocean waves can be used to continuously study the temperature and wind structure of the atmospheric boundary layer, troposphere, stratosphere, mesosphere, and lower thermosphere. Ocean-surface winds generate swells, which may interact nonlinearly to generate infrasound, which in turn may propagate for thousands of kilometers along the lower, middle, and upper atmosphere. Once these ocean swells reach a coastline, waves break and generate infrasound that may propagate along the boundary layer and lower atmosphere. Our studies suggest that a large portion of coherent microbarom arrivals observed in Hawaii are strongly affected by advection from the atmospheric winds in the 10–20 and 50–70 km height ranges. However, energetic swells can generate strong microbarom signals that may arrive from any direction, and may be refracted back to the ground at the thermosphere. By comparing the predicted atmospheric waveguide boundaries with the observed microbarom arrivals, we conclude that either (1) the wind speeds in the troposphere, stratosphere and mesosphere may be underestimated in atmospheric models or (2) elevated leaky infrasonic waveguides are persistent propagation paths that should be investigated in more detail. In particular, it would be valuable to study diffraction and scattering of infrasonic energy into and out of these postulated elevated waveguides.

Although in general the continuous microbarom noise is uncorrelated at I59US, distinct coherent microbarom packets can be routinely detected in the Hawaii array. When designing an array it may be useful to retain the coherence of microbaroms, as then it may then be possible to remove this contribution from a signal of interest and lower the background noise levels around the 0.2 Hz band. In principle, it may be also possible to individually extract coherent arrivals associated with open-ocean sources to yield signals refracted from different layers of the atmosphere and source regions. This may permit the identification of interesting transient reflection and refraction layers in the atmosphere as well as facilitate the recognition of microbarom signals produced by reflections from coastlines. Microbarom amplitude studies may yield further information on the variability of the atmospheric wind structure. There is also potential for using microbaroms to monitor ocean wave activity, since microbaroms contain information about the wave periods and amplitudes of the generating open ocean waves.

Although ocean swells have been previously used as a natural source for continuous measurements of atmospheric winds over long horizontal ranges, recent advances in measurement and modeling techniques can provide new insight on this complex but tractable method for continuous, passive acoustic tomography of the atmosphere.

ACKNOWLEDGEMENTS

Many thanks to Douglas Drob, NRL, and Alexis Le Pichon, CEA/DASE, for their collaboration on the study of the wind effects. Paul Wittmann (FNMOC) provided the guidance in getting WW3 operational for this research.

REFERENCES

Arendt, S., and D. Fritts, (2000) Acoustic radiation by ocean surface waves. *J. Fluid Mech*., 415, 1-21,

Benioff, H. and B. Gutenberg, (1939) Waves and currents recorded by electromagnetic barographs. *Bull. Am. Met. Soc*., 20, 421.

Cansi, Y, (1995) An automatic seismic event processing for detection and location: The P.M.C.C. method, *Geophys. Res. Lett., 22*, 1021-1024.

Cox, E., H Plagge, and J. Reed, (1954) Meteorology directs where blast will strike, *Bull. Amer. Meteorol. Soc*., 35.

Daniels, F. B., (1952) Acoustical energy generated by the ocean waves. *J. Acoust. Soc. Am*., 24, 83.

Daniels, F. B., (1942) Generation of infrasound by ocean waves. *J. Acoust. Soc. Am.*, 34, 352-353.

Donn, W. L. and B. Naini, (1973) Sea wave origin of microbaroms and microseisms. *J. Geophys. Res.,* 78, 4482-4488.

Donn, W. L. and E. S. Posmentier (1967) Infrasonic waves from the marine storm of April 7, 1966. *J. Geophys. Res.*, 72**,** 2053-2061.

Donn W. and D. Rind, (1971) Natural infrasound as an atmospheric probe, *Geophys, J. R. Astr. Soc*., 26, 111-133.

Drob, D., M. Picone, and M. Garcés, (2003) The Global Morphology of Infrasound Path Partitioning, *J. Geophys. Res*., 108, 4680.

Garcés, M., C. Hetzer, M. Merrifield, M. Willis, and J. Aucan. (2003) Observations of surf infrasound in Hawaii, *Geophys. Res. Letts.*, **30**(24), 2264.

Garcés, M., D. Drob, and M. Picone, (2002a) A theoretical study of the effect of geomagnetic fluctuations and solar tides on the propagation of infrasonic waves in the atmosphere. *Geophys. J. International*, 148, 77-87.

Garcés, M., C. Hetzer, K. Lindquist, and D. Drob. (2002b) Source Location Algorithm for Infrasonic Monitoring, *Proceedings of the 24th Seismic Research Review–Nuclear Explosion Monitoring*. 745-754.

Garcés, M., C. Hetzer, M. Willis, and S. Businger, (2003) Integration of infrasonic models with ocean wave spectra and atmospheric specifications to produce global estimates of microbarom signal levels. *Proceedings of the 25th Seismic Research Review–Nuclear Explosion Monitoring: Building the Knowledge Base,* 617-627.

Le Pichon, A., J. L. Plantet, Y. Cansi, J. Guilbert, P. Herry, S. Lambotte, (2003) Recent developments on infrasound data processing at the French NDC, *Proceedings of the Infrasound Technology Workshop*, San Diego, CA, 27–30 October 2003.

Madisetti, V. K. and D. B. Williams, (1998) *The Digital Processing Handbook.* CRC Press, Florida. 14-7pp..

Longuet-Higgins, H. C. (1950) A theory of the origin of microseisms, *Philos. Trans. Roy. Soc*., London Ser. A243, 1-35.

Ponomaryov E. A., A. G. Sorokin, and V. N. Tabulevich, (1998) Microseisms and infrasound: a kind of remote sensing. *Physics of the Earth and Planetary Interiors*, 108, 339-346.

Rind, D., (1980) Microseisms at Palisades 3. Microseisms and microbaroms, *J. Geophys. Res.*, 85, 4854-4862.

Sanderson, M. (Editor), (1993) *Prevailing Trade Winds*. Univ. of Hawaii Press, 12-36.

Saxer, L., (1945) Electrische Messung kleiner atmospharischer Druckshwankingen, *Helv. Phys. Acta.*, 18, 527.

Saxer, L., (1954) Über Entstehung und Ausbreitung quasiperiodischer Luftdruckschwankungen. *Arch. Meteorol. Geophys. Bioklum*., A6, 451-457.

Rind, D., (1978) Investigation of the lower thermosphere results of ten years of continuous observations with natural infrasound, J. of Atmospheric and Terrestrial Physics, 40, 1199-1209.

Tolman, H., B. Balasubramaniyan, L. Burroughs, D. Chalikov, Y. Chao, H. Chen, and V. Gerald, (2002) Development and implementation of ocean surface wave models at NCEP, *Weather and Forecasting*, 17, 311-333.

Tabulevich, V., (1995) On recordings of global microseismic vibrations and observations of microseisms in shore zones of oceans, *Physics of the Earth and Planetary Interiors*, 91, 299-305.

Willis, M., (2004) Observations and source modeling of microbaroms in the Pacific. Masters Thesis, Dept. of Meteorology, University of Hawaii at Manoa, 65 pp.

Wright, C. W., E. J. Walsh, D. Vandemark, W. B. Krabill, A. W. Garcia, S. H. Houston, M. D. Powell, P. G. Black, and F. D. Marks, (1998) Hurricane Directional Wave Spectrum Variation in the Open Ocean. *J. Phys. Oceanogr.*, 31, 2472-2488.

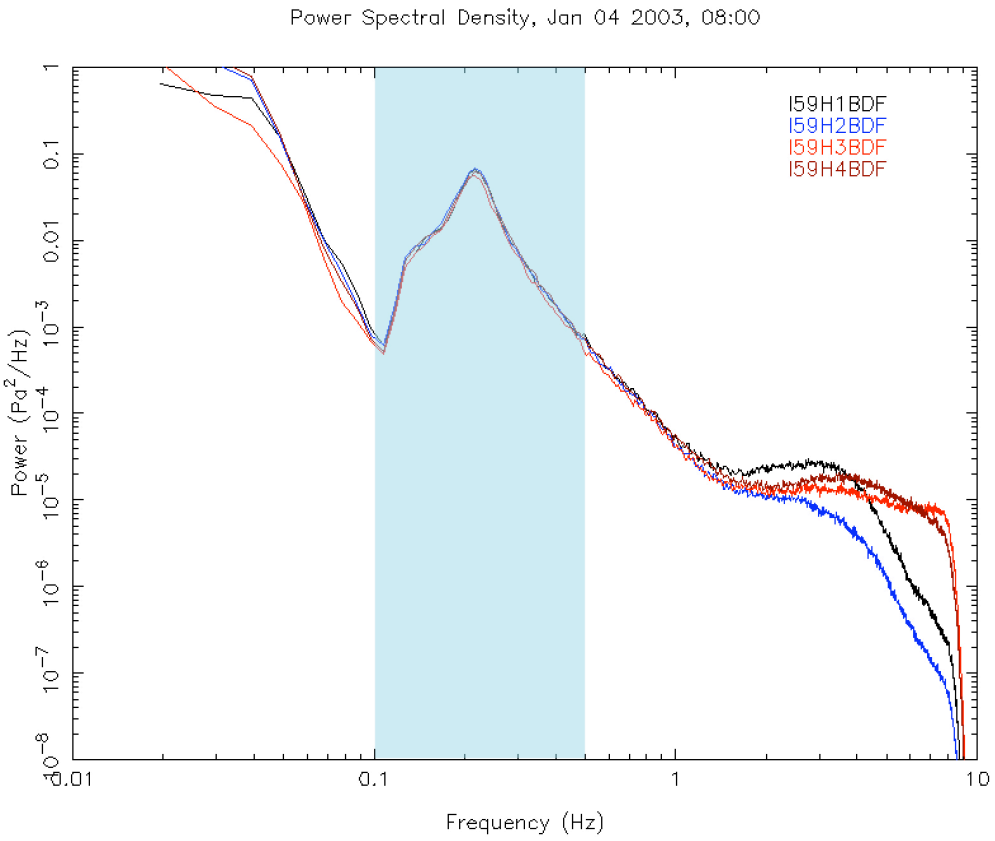

Figure 1. Infrasonic power spectral density observed at I59US site on January 4, 2003 18 UTC (8 AM local). Colored lines represent power observed by the four components of the infrasonic array. Power (Pa^2/Hz) is on the vertical axis, frequency (Hz) is on the horizontal axis. The blue-shaded region represents the microbarom-frequency range. The approximately 0.2-Hz peak is common throughout the year at I59US, which theoretically corresponds to ocean waves of 10 seconds.

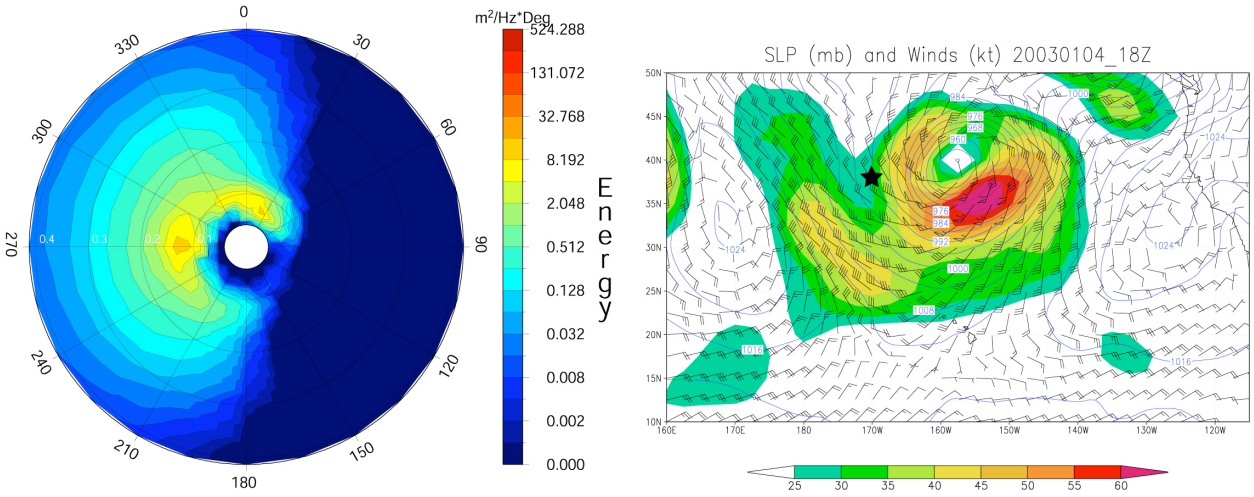

Figure 2. Polar plot (left) represents the directional ocean-wave spectrum for a grid point (38.00N, 170.00W) at 18 UTC on January 4, 2003 in the wake region of a strong marine storm shown in adjacent plot of sea-level pressure. Frequency (Hz) decreases towards the center, wave energy scale (m^2/Hz*deg) on the right hand side. This ocean-wave spectrum contains energy arriving from several directions and thus, microbarom generation is expected. The black star on the sea-level-pressure map represents the point of the wave spectrum. The wave spectrum was plotted using WW3 hindcast data. NCEP/NCAR Reanalysis data was used to generate the surface weather plot.

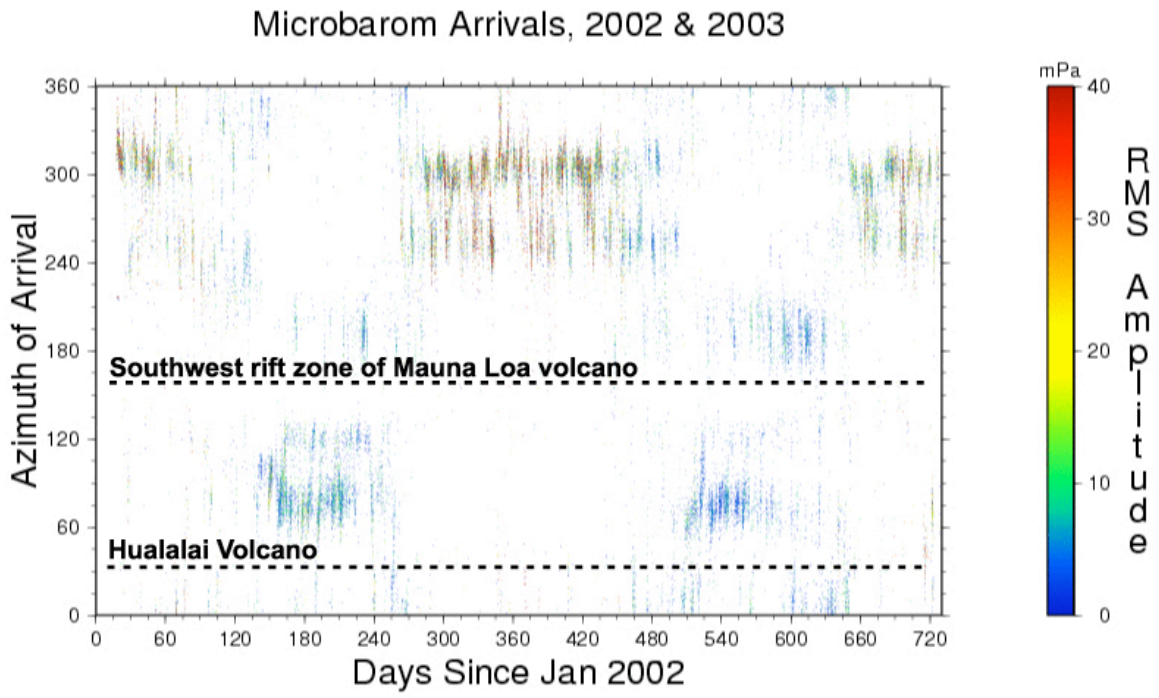

Figure 3. Infrasonic wave arrival azimuth and amplitude of coherent microbarom arrivals at I59US during 2003. Arrival azimuth at the array is measured clockwise from north (0° to 360°).

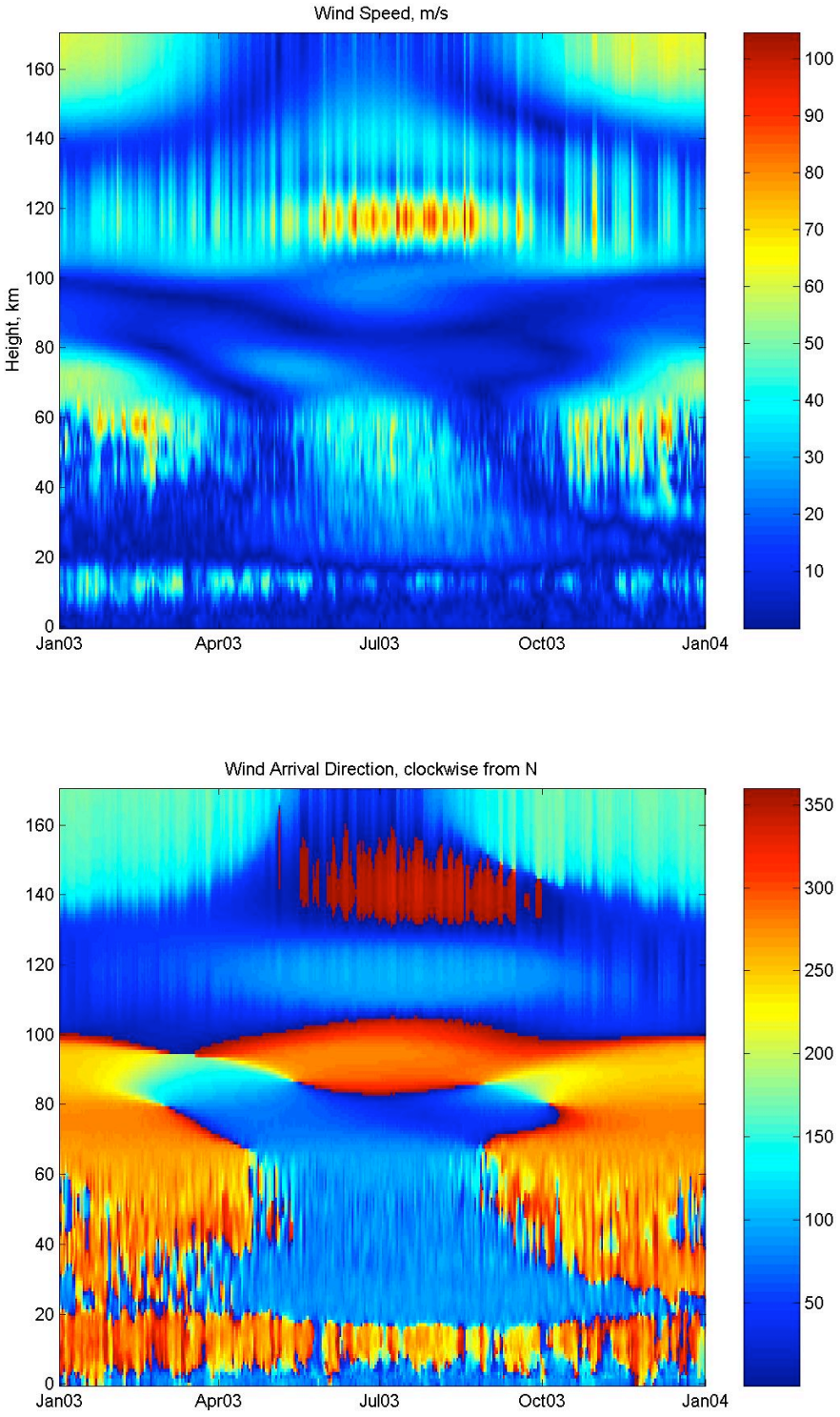

Figure 4. Wind-speed and direction as provided by the G2S atmospheric specifications over Hawaii for 2003 at 18 UTC.

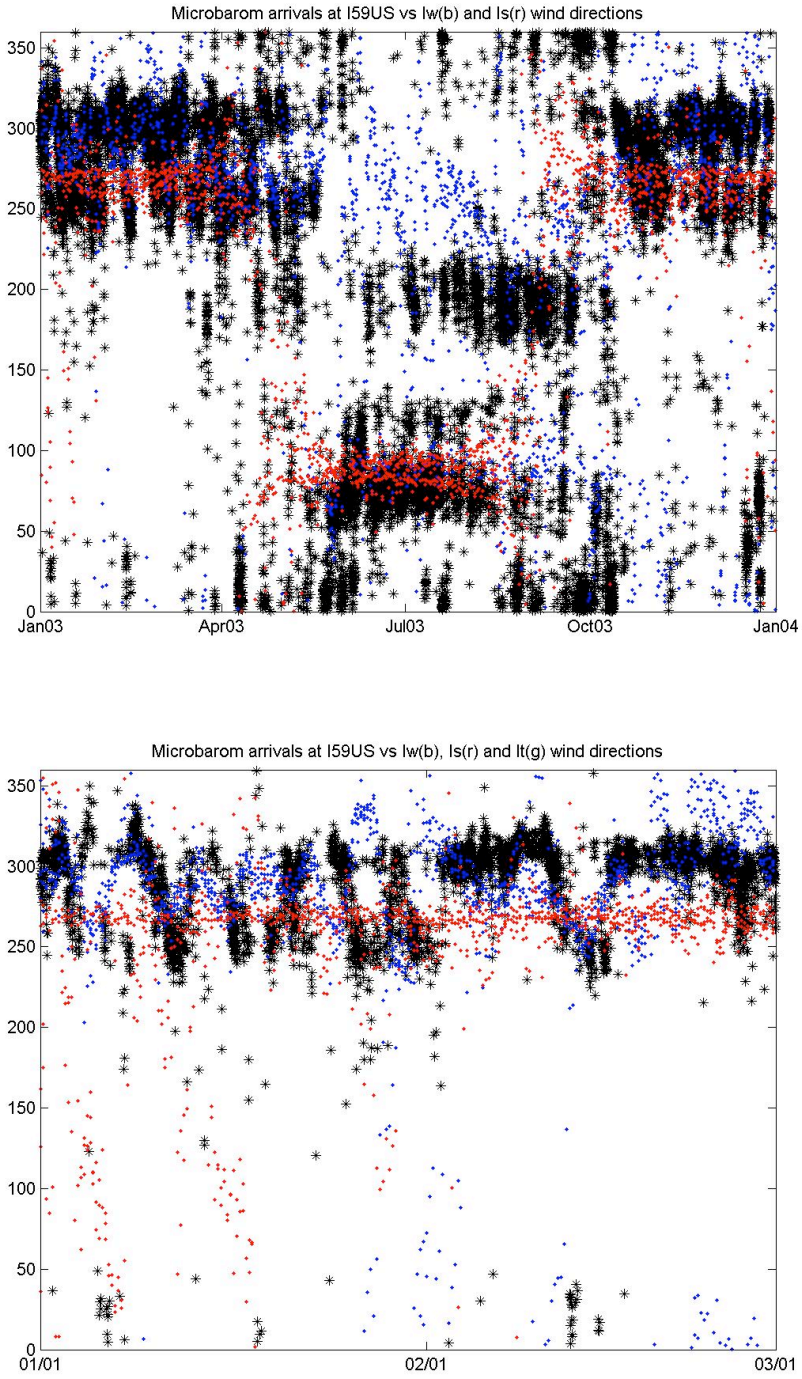

Figure 5. Coherent microbarom arrival and wind arrival azimuths, clockwise from north, at the Hawaii array. The red dots represent the winds between 50–70 km and the blue dots represent the winds between 10–20 kms. The dominant wind directions match the seasonal variability for some of the arrivals, except for the arrivals from the southern hemisphere during the Austral winter. These swells are large, consistent, and powerful, and may overwhelm the 10 second period swell energy.